

# Theoretical Study of Cation/Ether Complexes: Alkali Metal Cations with 1,2-Dimethoxyethane and 12-Crown-4

Susan E. Hill, David Feller,\* and Eric D. Glendening†

Environmental Molecular Sciences Laboratory, Pacific Northwest National Laboratory, 906 Battelle Blvd., MS K1-96, Richland, Washington 99352

Received: December 16, 1997; In Final Form: February 18, 1998

Hartree–Fock and second-order perturbation theory methods were used to determine structures and binding enthalpies of complexes formed from a single alkali metal cation ( $\text{Li}^+$  through  $\text{Cs}^+$ ) and one or two 1,2-dimethoxyethane ligands or 12-crown-4. These calculations employed multiple basis sets in order to determine the sensitivity of the results to the completeness in the one-particle basis. The results are compared with recently reported collision-induced dissociation experimental findings. In general, good agreement was found between the experimental and theoretical bond dissociation enthalpies, although for the heavier cations discrepancies of as much as 14 kcal/mol or more were uncovered. Possible reasons for these anomalies are discussed.

## I. Introduction

The class of cyclic molecules known as crown ethers<sup>1</sup> possesses the ability to bind specific metal cations in complex solutions of chemically similar ions. This characteristic has led to the widespread use of crowns as chemical separation agents. Their suitability for dealing with the high-level wastes on the Hanford nuclear reservation in Washington state is currently being examined.<sup>2</sup> Because of the scope of the radioactive contamination at this and similar sites around the world, there are strong economic incentives to improve the separation agent's ability to discriminate in favor of the target cation and to improve the ease with which the ligand incorporates the cation. Any progress in this direction rests upon a basic understanding of the relative importance of the variety of factors governing cation/ether interactions.

Much of the nuclear waste is dissolved in high-pH sludge in large underground storage tanks. Computational models<sup>3–17</sup> of the complex molecular processes occurring in solution and at the liquid/solid interface require a reliable body of both gas- and liquid-phase data upon which to draw. Empirical force fields, which serve as the foundation of aqueous-phase molecular dynamics simulations, must be calibrated against experiment or higher levels of theory.

Accurate experimental values of such fundamental quantities as gas-phase cation–ether bond dissociation enthalpies,  $\Delta H^{298}$ , would provide an ideal complement to theoretical predictions. Unfortunately, very few of the experimental studies conducted over the past several decades have attempted to measure this quantity.<sup>18–30</sup> One of the few that did is the work of Katritzky et al.<sup>20</sup> on 18-crown-6 (18c6). For reasons that were not clear, agreement with moderately high-level ab initio calculations was poor.<sup>31</sup> Very recently, a new collection of collision-induced dissociation (CID) measurements<sup>32–37</sup> of cation/ether bond enthalpies have appeared in the literature. These provide an important new comparison set for theory.

In the present work we report the results of an ab initio theoretical study of cation–ether complexes of the form:  $\text{M}^+(\text{DXE})_n$ ,  $n = 1$  or  $2$ , where  $\text{M} = \text{Li}, \text{Na}, \text{K}, \text{Rb}, \text{Cs}$  and DXE is 1,2-dimethoxyethane. We have also investigated complexes involving the 12-crown-4 (12c4) macrocycle. The current findings will be analyzed in light of the available CID experimental bond enthalpies and previously reported data for the related dimethyl ether ligand.<sup>32–34</sup> The behavior of complexes formed from these acyclic ethers will be contrasted with 12c4, where even the smallest of the alkali metals is too large to fit completely within the macrocycle cavity. By comparing our results with the CID values, we hope to improve our understanding of the cause of the disagreement between theory and experiment for the  $\text{K}^+:\text{18c6}$  and  $\text{Cs}^+:\text{18c6}$  complexes. The smaller size of the  $\text{M}^+(\text{DXE})_n$  complexes will permit higher levels of theory to be applied than would be possible with 18c6 or its derivatives.<sup>13,14,31,38</sup>

The physics of cation/ether interactions can be qualitatively described by a simple charge–charge/charge–dipole electrostatic model. For example, Hay and Rustad<sup>17</sup> have emphasized the importance of properly aligning the ether oxygen dipole moments in the direction of the metal cation, whereas traditionally the focus was on matching the cation's diameter to the crown cavity. This model implies that binding strength is primarily a function of (1) the number of available electron donor sites within the crown, (2) their basicity, (3) the distance separating the metal cation and the ether oxygens, and (4) the alignment of the dipoles. The last two effects are loosely associated with the issue of matching cation/crown size, but this simple model fails to include the crown distortion energy that may be required to optimize the electrostatics. Studies<sup>31</sup> have shown that the third factor dominates for gas-phase complexes. Thus, among the alkali cations 18c6 binds  $\text{Li}^+$  most strongly, because the  $\text{M}^+-\text{O}$  distance is the shortest, despite strain resulting from the folding of the macrocycle backbone. Binding decreases monotonically for each of the heavier alkali metals. The work of Glendening et al.<sup>31,38</sup> showed significant nonclassical contributions to binding from effects such as charge

† Current address: Department of Chemistry, Indiana State University, Terre Haute, Indiana 47809.

\* To whom correspondence should be addressed.

transfer, especially for the alkaline earth dications. A proper description of the cation's polarizability was also found to be important.

## II. Procedure

Bond dissociation enthalpies were computed for the  $M^+$ -(DXE)<sub>n</sub> and  $M^+ \cdot 12c4$  complexes by first optimizing the structures of the complexes at the restricted Hartree-Fock (RHF) level of theory. For this purpose a hybrid basis set consisting of 6-31+G\*<sup>39-41</sup> for oxygen and 6-31G\* for hydrogen, lithium, carbon, and sodium was used, equivalent to the basis set used in previous studies. K, Rb, and Cs were treated with effective core potentials (ECPs) from Hay and Wadt,<sup>42</sup> with core definitions that excluded the (*n* - 1) atomic shell, e.g., the potassium (3s, 3p) shell. A (5s, 5p) → [3s, 3p] contraction of the original Hay and Wadt functions was used for K, Rb, and Cs, with an additional six-term d-type polarization function. Polarization function exponents were optimized by Glendening et al.<sup>31</sup> for the  $M^+(H_2O)$  systems. Relativistic mass velocity and one-electron Darwin effects are incorporated into our rubidium and cesium calculations via the ECPs. For the sake of brevity, the overall collection of basis functions plus metal ECPs will be referred to as the 6-31+G\* basis set throughout this paper. Binding enthalpies at 298 K were obtained from standard gas-phase expressions<sup>43</sup> using either scaled RHF harmonic frequencies (scale factor = 0.9) or unscaled MP2 frequencies. All calculations were performed using Gaussian 92<sup>44</sup> and Gaussian 94,<sup>45</sup> with geometry optimizations satisfying a "tight" optimization criterion (maximum forces less than  $1.5 \times 10^{-5}$   $E_h/\text{bohr}$  and root-mean-square forces less than  $1.0 \times 10^{-5}$   $E_h/\text{bohr}$  on the atoms).

Because Hartree-Fock binding energies often underestimate the binding energies obtained from correlated calculations by 3–6 kcal/mol, second-order Møller-Plesset perturbation theory (MP2) calculations were performed at the RHF geometries. The (*n* - 1) shell of electrons on the metal cations were included in the correlation treatment. Undesirable basis set superposition error (BSSE) was minimized through use of the full counterpoise correction of Boys and Bernardi.<sup>46</sup>

The computational procedure described thus far corresponds exactly to the procedure used in our earlier studies of 18c6 and larger derivatives.<sup>35,47-49</sup> The use of larger basis sets or correlated methods to determine structures and frequencies would have been prohibitively expensive. However, the smaller size of the present complexes makes it possible to explore these effects. Therefore, for selected complexes we have reoptimized structures and recomputed bond enthalpies at the MP2 level using both the 6-31+G\* basis set and the larger aug-cc-pVDZ basis.<sup>50,51</sup> With the latter, a [6s, 5p, 2d] all-electron potassium basis set<sup>49</sup> was used instead of the Hay/Wadt ECP.

Even larger basis set calculations were performed on  $K^+$ -(DXE) in order to estimate the complete basis set (CBS) MP2 limit. These basis sets consisted of the correlation-consistent cc-pVTZ, cc-pVQZ, and aug-cc-pVTZ sets for H, C, and O and an [8s, 7p, 4d, 2f] basis for potassium.<sup>52</sup> The largest of these totaled 569 functions. A single-point MP2 energy evaluation required slightly more than 22 h on an SGI Origin 2000, running with four processors.

As noted previously,<sup>33</sup> DXE has two nearly degenerate conformers, which differ primarily in the dihedral twist angle about the central C-C bond. The lowest conformer is conventionally labeled ttt (or simply trans) and possesses  $C_{2h}$  symmetry. At the highest level of theory employed in that study (MP2/aug-cc-pVDZ), the second conformer (denoted trans-

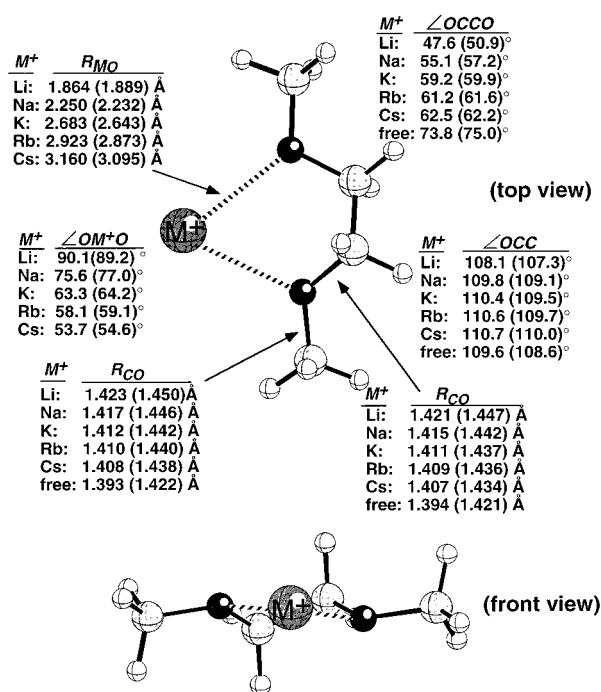


**Figure 1.** Optimized  $M^+$ -(DXE) structures ( $C_2$  symmetry) at the RHF/6-31+G\* and MP2/6-31+G\* (in parentheses) levels of theory. The Li data was taken from Ray et al.<sup>33</sup> MP2/aug-cc-pVDZ optimized metal-oxygen distances are: 1.901 (Li), 2.251 (Na), 2.653 (K), 2.866 (Rb), and 3.118 (Cs) Å.

gauche-trans) was only 0.2 kcal/mol higher in energy than the ttt conformer, ignoring zero-point vibrational effects. Zero-point energies for the two conformers are essentially identical. Reevaluating the energy difference at the coupled cluster level of theory, including single and double excitations plus a perturbative estimate of triple excitations (CCSD(T)), yields a slightly larger 0.5 kcal/mol gap. All energy differences involving DXE in the current study will be with respect to the ttt conformer.

## III. Results

**A.  $M^+$ -(DXE).** The optimized RHF and MP2 structural parameters for the lowest-energy ( $C_2$  symmetry) forms of  $M^+$ -(DXE) are shown in Figure 1. As expected, the largest variation occurs for the  $M^+$ -O bond lengths, which increase by nearly a factor of 2 across the  $Li^+ \rightarrow Cs^+$  sequence. Correlation recovery at the MP2 level increases  $R_{MO}$  by 0.02 Å in  $Li^+$ -(DXE) and decreases it by 0.02–0.07 Å in the other complexes. Similar behavior was noted for the corresponding complexes formed from dimethyl ether (DME).<sup>34</sup> The increase in  $R_{MO}$  gives rise to a corresponding decrease in the O-M<sup>+</sup>-O bond angle, despite the 12° opening of the O-C-C-O dihedral angle. Even for the largest cation, this dihedral angle is still 13° smaller than the optimal value for the uncomplexed DXE. For the smaller cations,  $R_{MO}$  is slightly longer in the  $M^+$ -(DXE) complexes than the corresponding distances in the related  $M^+$ -(DME)<sub>2</sub> complexes, using the same basis set and methods.<sup>32,34</sup> This lengthening is due to the constraints on the orientation of the ether dipoles imposed by the DXE backbone. For the heavier cations, the MO distances for the  $M^+$ -(DXE) and  $M^+$ -(DME)<sub>2</sub> complexes are nearly identical.

Total energies at the various levels of theory are listed in Table 1, and  $\Delta H^{298}$  values are provided in Table 2. Correlation recovery is somewhat more important for the larger, more polarizable cations than for the smaller ones. With the exception

**TABLE 1: RHF and MP2 Energies for  $M^+(\text{DXE})$ ,  $M^+(\text{DXE})_2$ , and  $M^+(\text{12c4})^a$** 

complex	basis	theory	geometry	Li	Na	K	Rb	Cs
$M^+(\text{DXE})$	6-31+G*	RHF	RHF/6-31+G*	-314.3253 <sup>b</sup>	-468.7164	-334.7397	-330.4693	-326.4982
		MP2	RHF/6-31+G*	-315.2054 <sup>b</sup>	-469.6027	-335.6952	-331.3843	-327.4172
		MP2	MP2/6-31+G*	-315.2083	-469.6057	-335.6982	-331.3874	-327.4204
	aVDZ est CBS <sup>c</sup>	MP2	MP2/aVDZ	-315.3463	-469.9367	-907.2324	-331.5712	-327.5754
$M^+(\text{DXE})_2$	6-31+G*	RHF	RHF/6-31+G*	-621.3784 <sup>b</sup>	-775.7557	-641.7160	-637.4864	-633.5100
		MP2	RHF/6-31+G*	-623.1468	-777.5302	-643.6036	-639.2863	-635.3138
$M^+(\text{12c4})$	6-31+G*	RHF	RHF/6-31+G*	-619.0404 <sup>b</sup>	-773.4245	-639.4331	-635.1636	-631.1891
		MP2	RHF/6-31+G*	-620.7972 <sup>b</sup>	775.1898	-641.2690	636.9590	-632.9887
	aVDZ	MP2	MP2/aVDZ			-1212.9305		

<sup>a</sup> Energies are given in hartrees. Frozen cores included the 1s orbital on Li, C, O, and Na, the (1s, 2s, 2p) orbitals on K, the (1s, 2s, 2p, 3s, 3p, 3d) orbitals on Rb, and the (1s, 2s, 2p, 3s, 3p, 3d, 4s, 4p, 4d) orbitals on Cs. The "aVDZ" basis label refers to the aug-cc-pVDZ basis set. Atomic 6-31+G\* energies are the following: Li<sup>+</sup>, -7.2355 (RHF); Na<sup>+</sup>, -161.6593 (RHF), -161.6609 (MP2); K<sup>+</sup>, -27.7056 (RHF), -27.7750 (MP2); Rb<sup>+</sup>, -23.4435 (RHF), -23.4729 (MP2); Cs<sup>+</sup>, -19.4790 (RHF), -19.5121 (MP2). Atomic VDZ energies are the following: Li<sup>+</sup>, -7.2361 (RHF); Na<sup>+</sup>, -161.8552 (MP2); K<sup>+</sup>, -599.1700 (MP2); Rb<sup>+</sup>, -23.5166 (MP2); Cs<sup>+</sup>, -19.5387 (MP2). <sup>b</sup> D. Ray et al.<sup>32</sup> <sup>c</sup> Estimated complete basis set value obtained from an exponential fit of the cc-pVDZ through cc-pVQZ MP2 energies.

**TABLE 2: Theoretical and Experimental Binding Enthalpies for  $M^+(\text{DXE})$ ,  $M^+(\text{DXE})_2$ , and  $M^+(\text{12c4})^a$** 

complex	basis	theory	geometry	binding enthalpy $\Delta H^{298}$				
				Li	Na	K	Rb	Cs
$M^+(\text{DXE})$	6-31+G*	RHF	RHF/6-31+G*	-61.9	-42.0	-28.6	-23.4	-19.3
		MP2	RHF/6-31+G*	-61.7	-42.9	-31.5	-26.2	-22.4
		MP2	MP2/6-31+G*	-61.6	-42.5	-31.3	-26.1	-22.3
	aVDZ est CBS <sup>b</sup> CID expt <sup>c</sup>	MP2	MP2/aVDZ	-59.2	-41.7	-30.0	-25.1	-21.5
		MP2	MP2/VTZ			-32.0		
			-59 ± 4	-39 ± 1	-29 ± 1	-23 ± 2	-14 ± 1	
$M^+(\text{DXE})_2$	6-31+G*	RHF	RHF/6-31+G*	-37.5	-29.5	-20.9	-17.2	-14.0
		MP2	RHF/6-31+G*	-40.7	-31.4	-23.7	-19.8	-16.7
	CID expt <sup>c</sup>			-33 ± 3	-27 ± 2	-20 ± 3	-11 ± 3	-12 ± 2
$M^+(\text{12c4})$	6-31+G*	RHF	RHF/6-31+G*	-88.2	-63.4	-44.7	-36.9	-30.8
		MP2	RHF/6-31+G*	-85.7	-61.7	-46.9	-39.1	-33.5
	aVDZ CID expt <sup>c</sup>	MP2	MP2/aVDZ			-45.8		
				-90 ± 12	-61 ± 3	-46 ± 3	-23 ± 3	-21 ± 2

<sup>a</sup> Binding enthalpies (in kcal/mol) for the 6-31+G\* basis set were corrected for the effects of basis set superposition error. The energies listed in the row labeled " $M^+(\text{DXE})_2$ " correspond to incremental binding energies for the process  $M^+(\text{DXE})_2 \rightarrow M^+(\text{DXE}) + \text{DXE}$ . The "aVDZ" basis set label refers to the aug-cc-pVDZ basis set for H, C, and O. The sodium basis set was cc-pCVDZ. The lithium data are taken from D. Ray et al.<sup>32</sup> Experimental uncertainties are ± 1 standard deviation. <sup>b</sup> Estimated complete basis set value obtained from the average of the cc-pVQZ and aug-cc-pVTZ MP2 binding enthalpies. <sup>c</sup> Collision-induced dissociation experimental data are taken from (Li) D. Ray et al.,<sup>32</sup> (Na) M. B. More et al.,<sup>34</sup> (K) M. B. More et al.,<sup>35</sup> and (Rb) and (Cs) M. B. More et al.<sup>36</sup>

of the CID results for Cs<sup>+</sup>, all of the experimental and theoretical  $M^+(\text{DXE})$  bond dissociation enthalpies are in good agreement with each other. The reason for the disagreement in the case of Cs<sup>+</sup> is not immediately obvious, since there was nearly perfect agreement between theory and experiment for the dissociation energy of Cs<sup>+</sup>(DME), and the theoretical value fell within the experimental error bars for Cs<sup>+</sup>(DME)<sub>2</sub>. The interpretation of the CID experiment is difficult. It involves a consideration of such factors as highly excited reactants, multiple collisions between the complex and the collision gas (Xe), and the finite lifetime of the dissociating complex.

On the theoretical side, none of the factors we examined produced a significant difference in our predicted values of  $\Delta H$ . Although BSSE for the smaller 6-31+G\* basis set was on the order of 5 kcal/mol at the MP2 level, the counterpoise correction brought the binding enthalpies back into good agreement with the larger aug-cc-pVDZ basis set results. Optimization of the  $M^+(\text{DXE})$  geometries at the MP2 level lowered their energies by several kcal/mol, but the differential effect on the dissociation enthalpies was ≤ 0.4 kcal/mol. All of the aug-cc-pVDZ values in Table 2 are 1–2 kcal/mol smaller than the 6-31+G\* values, but the complete basis set limit for the  $\Delta H^{298}$  of K<sup>+</sup>(DXE) is similarly 2 kcal/mol larger than the aug-cc-pVDZ value. To the extent this result is indicative of the trend for the other cations, we would estimate that the MP2/6-31+G\* binding

enthalpies are within about 1.5 kcal/mol of the CBS limits. This is likely due to a fortuitous cancellation of error, since the 6-31+G\* basis set is known to produce nontrivial errors in the polarizabilities of the cations and the dipole moments of the ligands.

Convergence of the K<sup>+</sup>(DXE) binding energy to the complete basis set limit is shown in Figure 2 for the cc-pVxZ and aug-cc-pVxZ basis set sequences. If we correct the cc-pVDZ and aug-cc-pVDZ MP2 binding energies for the effects of BSSE, the resulting values are in poorer agreement with the apparent CBS limit, which lies near -32.5 kcal/mol, than the uncorrected energies. This observation, as well as similar observations for K<sup>+</sup>(DME)<sup>34</sup> and  $M^+(\text{H}_2\text{O})_n$  clusters, suggests that for cationic clusters in general the counterpoise correction does not lead to improved agreement with the CBS limit for the correlation-consistent basis sets.

Mulliken population analyses of the  $M^+(\text{DXE})$  complexes show pronounced charge transfer for the smaller cations, amounting to 0.3 e<sup>-</sup> for Li and 0.1 e<sup>-</sup> for Na, whereas Cs<sup>+</sup> shows only a 0.04 e<sup>-</sup> transfer from the ether oxygens. A natural energy decomposition analysis (NEDA)<sup>53</sup> attributes 24 kcal/mol of attractive interaction to O → M<sup>+</sup> charge transfer in the Li<sup>+</sup>(DXE) complex. Although the magnitude of the attractive electrostatic contribution to the binding energy decreases with decreasing binding strength along the Li<sup>+</sup> to Cs<sup>+</sup> sequence, the

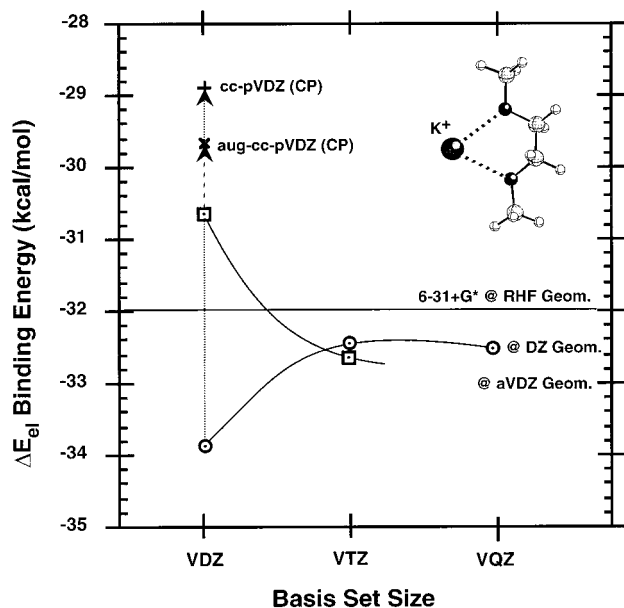


**Figure 2.** Basis set convergence for the binding energy of  $K^+(DXE)_2$  at the MP2 (core/valence) level of theory. The counterpoise-corrected values of the binding energy are indicated by + (cc-pVDZ) and × (aug-cc-pVDZ).

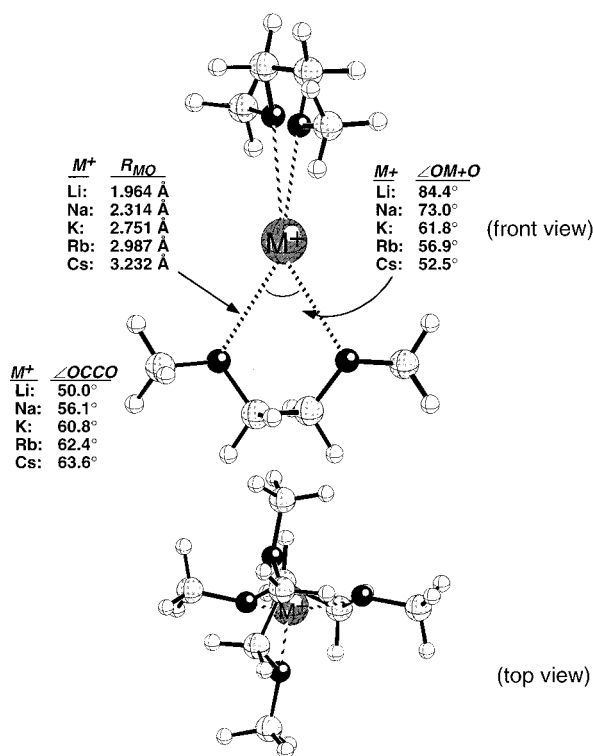


**Figure 3.** Optimized  $M^+(DXE)_2$  structures ( $S_4$  symmetry) at the RHF/6-31+ $G^*$  level of theory. The Li data were taken from Ray et al.<sup>33</sup>

relative contribution to the total binding energy is nearly independent of the type of metal or ligand type for complexes containing the same number of oxygens.

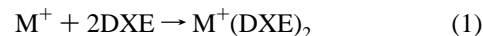
**B.  $M^+(DXE)_2$ .** The RHF/6-31+ $G^*$  optimized geometries of the  $M^+(DXE)_2$  complexes are shown in Figure 3. The lowest-energy conformers were found to possess  $S_4$  symmetry. A reduction in the metal cation charge caused by charge transfer from the first DXE ligand and  $DXE \leftrightarrow DXE$  repulsion results in a lengthening of the  $M^+-O$  distances relative to their values in  $M^+(DXE)$ . The effect is most pronounced for the smallest cation ( $Li^+$ ), with an increase in  $R_{MO}$  of 0.1 Å. Trends across

the  $Li^+$  to  $Cs^+$  sequence for the geometric parameters shown in Figure 3 are qualitatively similar to what was observed for  $M^+(DXE)$ .

$M^+(DXE)_2$  can be compared with the related quadridentate complex  $M^+(DME)_4$ , in which the four aliphatic ether donors have greater freedom to orient themselves about the central metal. The  $M-O$  distances for  $M^+(DXE)_2$  and  $M^+(DME)_4$  are identical, to within 0.01 Å, with the exception of  $Li^+$ .<sup>34</sup> Lithium is sufficiently small such that the steric repulsion between the DME ligands results in  $Li-O$  distances that are 0.03 Å longer than the values for  $Li^+(DXE)_2$ .<sup>32</sup>

As noted previously,<sup>34</sup> the use of effective core potentials for weakly bound systems can give rise to spurious imaginary frequencies owing to the need for numerical difference techniques for computing second derivatives in codes such as Gaussian 94. Specifically, the  $Rb^+(DXE)_2$  and  $Cs^+(DXE)_2$  complexes exhibit small imaginary frequencies that we consider to be numerical noise. The RHF optimized structure for  $Rb^+(DXE)_2$  has two imaginary frequencies (3.7i and 0.6i) and  $Cs^+(DXE)_2$  has three (5.5i, 5.3i, and 3.4i). We have shown previously that resorting to an MP2 optimization will eliminate these imaginary frequencies, but that the impact on binding energetics is negligible.

We have chosen to define the total binding energy of  $M^+(DXE)_2$  as the energy change associated with the reaction



where a counterpoise correction was made for each of the three reactants using the complex's geometry. The incremental binding energy of  $M^+(DXE)_2$  is then taken to be the difference in total binding energies of  $M^+(DXE)$  and  $M^+(DXE)_2$ .

In general, the agreement between the counterpoise-corrected MP2 and CID experimental binding enthalpies ( $M^+(DXE)_2 \rightarrow M^+(DXE) + DXE$ ) is worse than it was for the  $M^+(DXE)$  bidentate complexes (see Table 2). Only  $Na^+$  and  $K^+$  are reasonably close. For the other three complexes, the threshold CID values are 20–40% smaller than the theoretical values. If we attempt to normalize the error by dividing the difference between theory and experiment by the number of metal–oxygen interactions, we arrive at a different perspective. The average unsigned error per  $M^+-O$  interaction for the  $M^+(DXE)$  complexes is 2.1 kcal/mol, compared with 1.5 kcal/mol for the  $M^+(DXE)_2$  complexes.

**C.  $M^+(12c4)$ .** The cavity in 12c4 is too small to accommodate any of the cations considered in this study. As seen in Figure 4 where the RHF/6-31+ $G^*$  optimized structures for  $M^+(12c4)$  are shown, all of the alkali metals sit atop the crown. The crown is folded in such a way as to allow each of the four ether dipoles to point toward the cation in a  $C_4$  configuration. The height of the cation above the oxygen plane varies from 0.71 Å for  $Li^+$  to 2.54 Å for  $Cs^+$ . The  $Li-O$  distance, which is the only distance to show appreciable change between  $Li^+(DXE)_2$  and  $Li^+(12c4)$ , is 0.04 Å longer in the latter.

The binding energies for the  $M^+(12c4)$  complexes are taken relative to the lowest energy  $S_4$  conformation of the crown. A variety of ab initio, semiempirical, and molecular mechanics calculations have all shown this conformer to be the global minimum.<sup>49,54</sup> As seen in Table 2,  $Li^+(12c4)$  is the only case where the magnitude of the CID experimental binding enthalpy exceeds the theoretical value. This may not be significant, since the experimental error bars are quite large ( $\pm 12$  kcal/mol). MP2 calculations on  $K^+(12c4)$  with the much larger aug-cc-pVDZ basis set show very little difference with the MP2/6-31+ $G^*$

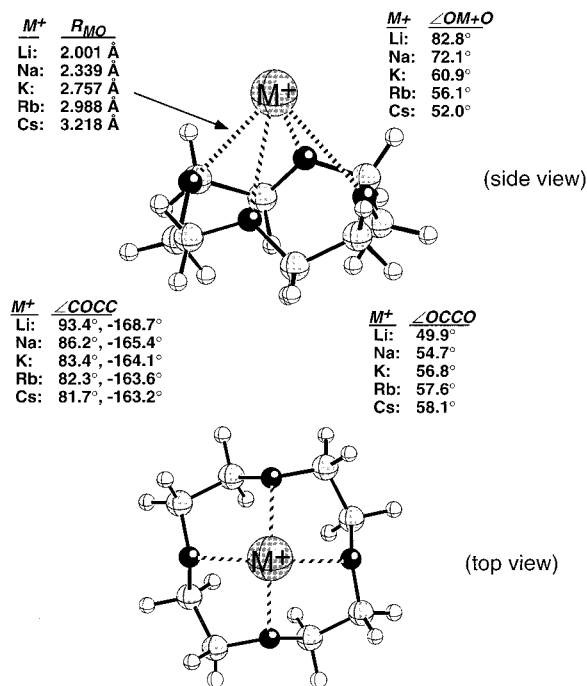


**Figure 4.** Optimized  $M^+(12c4)$  structures ( $C_4$  symmetry) at the RHF/6-31+ $G^*$  level of theory. The Li data were taken from Ray et al.<sup>33</sup>

counterpoise-corrected value. At 435 functions, these were the largest correlated geometry optimizations performed in this study.

The discrepancy between theory and experiment is unusually large for Rb (16 kcal/mol) and Cs (13 kcal/mol). More et al.<sup>37</sup> have discussed possible sources of error in the interpretation of the CID data. Of these, they concluded that overestimating the lifetime of the activated complex prior to dissociation was unlikely. Another explanation for the anomalously low experimental binding enthalpies was the possibility that a significant number of complexes were trapped in a higher-energy conformation. Given a mixture of  $M^+(12c4)$  complexes, some in the minimum energy conformation and others in a higher-lying conformation, the dissociation threshold detected by the CID experiment would correspond to the least strongly bond conformer.

Although a detailed examination of the case for higher-lying conformers as the source of the disagreement between theory and experiment is beyond the scope of the present work, we were able to identify MP2/6-31+ $G^*$   $C_{2v}$  symmetry conformers of  $K^+$ ,  $Rb^+$ , and  $Cs^+$  (see Figure 5) that lie 13–14 kcal/mol higher in energy than the  $C_4$  global minima. In this higher-lying conformation, the 12c4 ring resembles the  $S_4$  global minimum structure of the isolated crown. Two ether oxygens point toward the cation and two point away. Subtracting 14 kcal/mol from the  $C_4$  binding enthalpies listed in Table 2 yields -33 (K), -25 (Rb), and -22 (Cs) kcal/mol. In the case of  $Rb^+$  and  $Cs^+$  this brings the theoretical value into much better agreement with the experimental values ( $-23 \pm 3$  and  $-21 \pm 3$  kcal/mol). However, for K the change in binding enthalpy significantly worsens the agreement with experimental results. The fact that the energy gap between all three  $C_{2v}$  complexes in Figure 5 and their respective global minima were essentially the same came as something of a surprise. In general, the smaller the cation, the shorter the  $M^+-O$  bond length and the stronger the interaction. We expected to find that two of the MO distances, corresponding to the oxygens pointed away from the cation, would be lengthened. Although that was the case

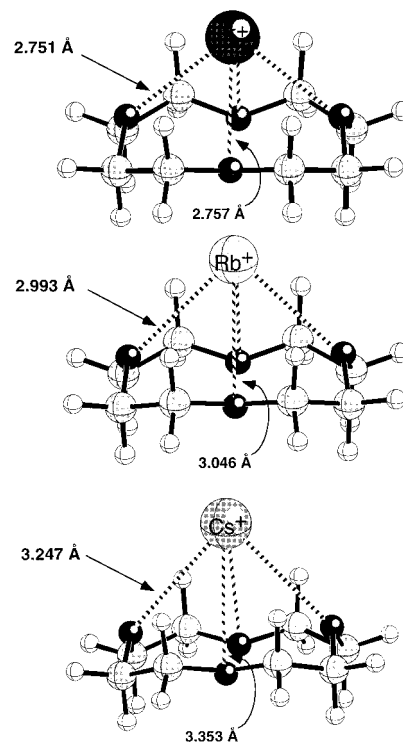


**Figure 5.** Optimized  $K^+(12c4)$ ,  $Rb^+(12c4)$ , and  $Cs^+(12c4)$  structures ( $C_{2v}$  symmetry) at the RHF/6-31+ $G^*$  level of theory.

for  $Rb^+(12c4)$  and  $Cs^+(12c4)$ , the  $K^+$  complex actually showed a slight decrease (0.006 Å) in two of the metal–oxygen distances and no change in the other two, compared with the  $R_{MO}$  values shown in Figure 4.

To invoke the higher-lying conformations of  $Rb^+(12c4)$  and  $Cs^+(12c4)$  as a possible explanation for the differences in the theoretical and experimental binding enthalpies, it is necessary to rationalize the apparently good agreement for  $K^+(12c4)$ , for which a similar high-lying conformation exists. It may be that the  $Rb^+(12c4)$  and  $Cs^+(12c4)$  complexes possess significantly higher barriers separating the  $C_{2v}$  and  $C_4$  conformations, whereas the strength of the  $K \leftrightarrow 12c4$  interaction is such that the barrier would be much smaller.

Identifying the transition state or multiple transition states connecting the  $C_4$  and  $C_{2v}$  structures is computationally very challenging because of the size of the basis set and the lack of analytical algorithms for computing second derivatives in our computer codes. A cruder approach to estimating the size of the barrier was made in the following manner. The interconversion of the  $C_4$  and  $C_{2v}$  structures principally involves a change in OCCO dihedral angles such that the two ether oxygens that point away from the metal in the  $C_{2v}$  conformation are rotated to point toward the cation. This change could occur via a concerted motion of the two oxygens or, in a stepwise fashion, one oxygen at a time. A rough estimate of the barrier height in the former case was found by following a linear synchronous transit (LST) between the two configurations of the heavy atom ring. The positions of the hydrogen atoms and the Rb cation were optimized. This procedure led to nearly identical barriers of  $\sim 11$  kcal/mol relative to the  $C_{2v}$  structure for all three cations ( $K^+$ ,  $Rb^+$ , and  $Cs^+$ ).

We were also able to identify minima in which three oxygens pointed toward the metal cation and one pointed away. The resulting potential energy surface is shown schematically in Figure 6. Here again, all three complexes were approximately the same energy (8 kcal/mol) above their respective global

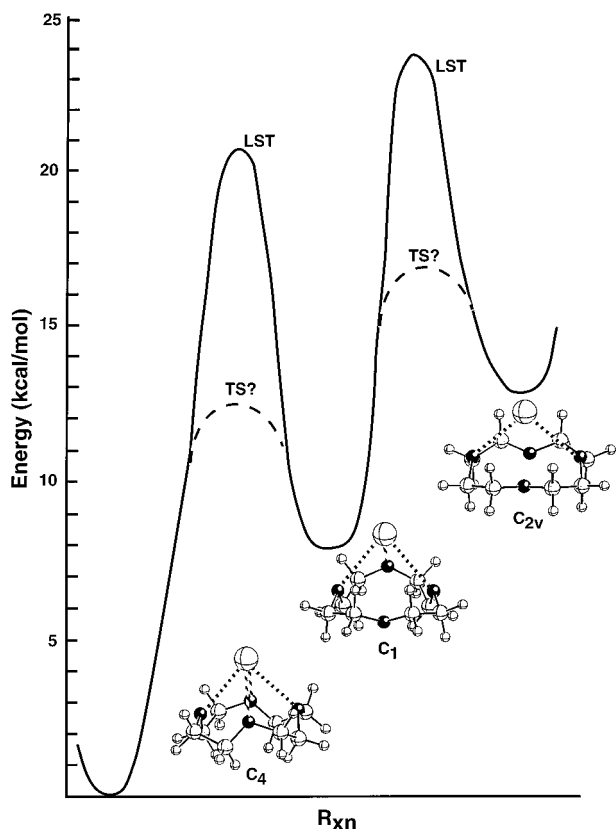


**Figure 6.** Schematic representation of the three  $\text{Rb}^+(12c4)$  conformations. Energies and geometries were obtained at the RHF/6-31+G\* level.

minima and the LST barriers were approximately the same height ( $\sim 11$  kcal/mol above the  $C_{2v}$  minima). It should be emphasized that the actual transition states may lie much lower in energy than the LST maxima. Thus, although we have identified higher-lying conformers for K, Rb, and Cs, we have not been able to uncover theoretical evidence that would explain why the  $\text{K}^+(12c4)$   $C_{2v}$  structure does not adversely affect the observed CID threshold, where excellent agreement between theory and experiment is found.

In their work on crown ethers, Hay and Rustad<sup>17</sup> have emphasized the importance of aligning the ether dipole toward the cation. In complexes formed from a single DME ligand, the metal is considered to achieve an "ideal" distance and orientation relative to the oxygen electron donor. With this as a reference point, one can obtain a qualitative estimate of the strain energy associated with the complexes discussed in this work. The M–O stretch and bend potentials for  $\text{Li}^+(\text{DME})$  and  $\text{Cs}^+(\text{DME})$  are shown in Figure 7. The surfaces are geometry-relaxed at the RHF/6-31+G\* level of theory. Metal–oxygen distances for  $\text{M}^+(\text{DXE})_{1-2}$  and  $\text{M}^+(12c4)$  complexes can be found in Figures 1, 3, and 4. Values of the two bend angles ( $\tau$  and  $\phi$ ) for the same complexes are shown in the lower half of Figure 7.

M–O stretch force constants derived from a combination of ab initio STO-3G potentials and M–O distances in the crystal structures are found by Hay and Rustad<sup>17</sup> to be smaller than the values predicted by RHF/6-31+G\* calculations. For example, the MM3 metal–oxygen force constants developed by Hay and Rustad range from 0.290 to 0.125 mdyn/Å (Li to Cs), whereas RHF/6-31+G\* predicts 1.13 to 0.25 mdyn/Å. The molecular mechanics force constants were derived by minimizing the error in computed metal–oxygen distances for a set of

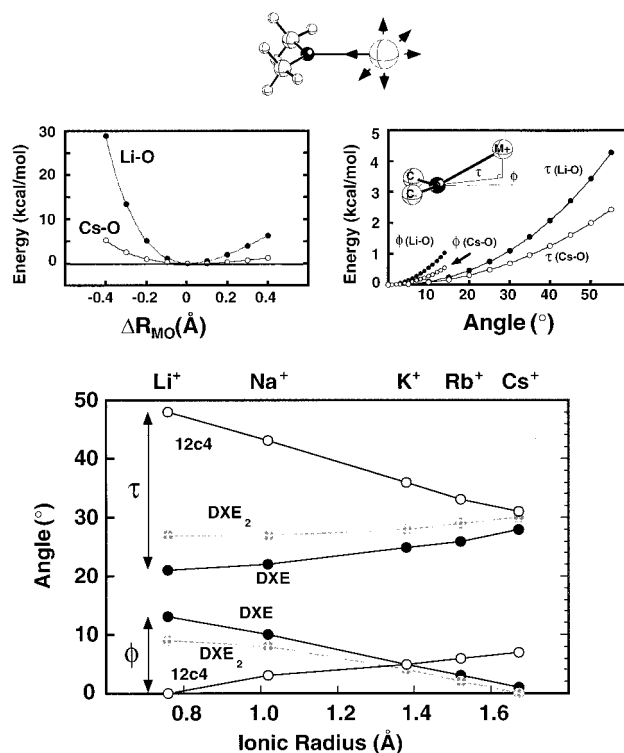


**Figure 7.** Upper plots show the M–O relaxed stretching potentials and the M–O–C relaxed bending potentials for  $\text{Li}^+(\text{DME})$  and  $\text{Cs}^+(\text{DME})$ . The out-of-plane tilt is denoted  $\tau$ , and the bend away from the perpendicular bisector plane is denoted  $\phi$ . The lower plot shows the M–O–C bend angles, relative to the planar configuration of the metal and the C–O–C ether functional group for  $\text{M}^+\text{L}$  (L = DXE, DXE<sub>2</sub>, and 12c4), as a function of increasing cation radius.

crystal structures, with the additional constraint that the force constants should smoothly decrease as the size of the cation increases.

#### IV. Summary and Conclusions

Structures and binding enthalpies of complexes formed from a single alkali metal cation ( $\text{Li}^+$  through  $\text{Cs}^+$ ) and one or two 1,2-dimethoxyethane ligands or 12-crown-4 have been computed using Hartree–Fock wave functions or second-order perturbation theory. A range of basis sets was used in order to probe the convergence of the results with respect to the basis set completeness. The results are compared with recently reported threshold CID experimental results. Although good agreement was found in general, experimental and theoretical bond dissociation enthalpies for the heavier cations sometimes differed by as much as 14 kcal/mol or more. Higher-lying conformers of  $\text{Rb}^+(12c4)$  and  $\text{Cs}^+(12c4)$  were identified as possible causes for the discrepancy between theory and experiment for these species.

**Acknowledgment.** This research was supported by the U.S. Department of Energy under Contract No. DE-AC06-76RLO 1830. The authors thank Dr. Kirk Peterson for a critical reading of this manuscript prior to publication. The authors also acknowledge the support of the Division of Chemical Sciences, Office of Basic Energy Sciences. S.E.H. and E.D.G. also acknowledge the support of the Associated Western Universities, Inc. (on behalf of Washington State University) under Grant No. DE-FG06-89ER-75522 with the U.S. Department of Energy. Portions of this work were completed on the computer resources at the National Energy Research Supercomputer Center with a

grant provided by the Scientific Computing Staff, Office of Energy Research, U.S. Department of Energy. The Pacific Northwest National Laboratory is a multiprogram national laboratory operated by Battelle Memorial Institute.

## References and Notes

- (1) Pedersen, C. J. *J. Am. Chem. Soc.* **1967**, *89*, 7017–7036.
- (2) Horwitz, E. P.; Dietz, M. L.; Fisher, D. E. *Solvent Extr. Ion Exch.* **1991**, *9*, 1.
- (3) Pullman, A.; Giessner-Prettre, C.; Kruglyak, Y. V. *Chem. Phys. Lett.* **1975**, *35*, 156–160.
- (4) Yamabe, T.; Hori, K.; Akagi, K.; Fukui, K. *Tetrahedron* **1979**, *35*, 1065–1072.
- (5) Hori, K.; Yamada, H.; Yamabe, T. *Tetrahedron* **1983**, *39*, 67–73.
- (6) Hannongbua, S. V.; Rode, B. M. *Inorg. Chem.* **1985**, *24*, 2577–2580.
- (7) Hase, W. L.; Richou, M.-C.; Mondro, S. L. *J. Phys. Chem.* **1989**, *93*, 539–545.
- (8) Badertscher, M.; Musso, S.; Welti, M.; Pretsch, E.; Maruizumi, T.; Ha, T.-K. *J. Comput. Chem.* **1990**, *11*, 819–828.
- (9) Ha, Y. L.; Chakraborty, A. K. *J. Phys. Chem.* **1992**, *96*, 6410–6417.
- (10) Leuwerink, F. T. H.; Harkema, S.; Briels, W. J.; Feil, D. *J. Comput. Chem.* **1993**, *14*, 899–906.
- (11) von Szentpály, L.; Shamovsky, I. L. *J. Mol. Struct.: THEOCHEM* **1994**, *305*, 249–260.
- (12) Wasada, H.; Tsutsui, Y.; Yamabe, S. *J. Phys. Chem.* **1996**, *100*, 7367–7371.
- (13) Feller, D. *J. Phys. Chem. A* **1997**, *101*, 2723.
- (14) Feller, D.; Thompson, M. A.; Kendall, R. A. *J. Phys. Chem. A* **1997**, *101*, 7292.
- (15) Thompson, M. A.; Glendening, E. D.; Feller, D. *J. Phys. Chem.* **1994**, *98*, 10465–10476.
- (16) Hay, B. P.; Rustad, J. R.; Hostetler, C. J. *J. Am. Chem. Soc.* **1993**, *115*, 11158–11164.
- (17) Hay, B. P.; Rustad, J. R. *J. Am. Chem. Soc.* **1994**, *116*, 6316–6326.
- (18) Liou, C.-C.; Brodbelt, J. S. *J. Am. Chem. Soc.* **1992**, *114*, 6761–6764.
- (19) Maleknia, S.; Brodbelt, J. *J. Am. Chem. Soc.* **1992**, *114*, 4295–4298.
- (20) Katritzky, A. R.; Malhotra, N.; Ramanathan, R.; Kemerait, R. C., Jr.; Zimmerman, J. A.; Eyler, J. R. *Rapid Commun. Mass Spectrom.* **1992**, *6*, 25–27.
- (21) Maleknia, S.; Brodbelt, J. *J. Am. Chem. Soc.* **1993**, *115*, 2837–2843.
- (22) Chu, I.-H.; Zhang, H.; Dearden, D. V. *J. Am. Chem. Soc.* **1993**, *115*, 5736–5744.
- (23) Brodbelt, J. S.; Liou, C.-C. *Pure Appl. Chem.* **1993**, *65*, 409–414.
- (24) Wu, H.-F.; Brodbelt, J. S. *J. Am. Chem. Soc.* **1994**, *116*, 6418–6426.
- (25) Liou, C.-C.; Wu, H.-F.; Brodbelt, J. S. *J. Am. Soc. Mass Spectrom.* **1994**, *5*, 260–273.
- (26) Wu, H.-F.; Brodbelt, J. S. *J. Inclusion Phenom.* **1994**, *18*, 37–44.
- (27) Wong, P. S. H.; Antonio, B. J.; Dearden, D. V. *J. Am. Soc. Mass Spectrom.* **1994**, *5*, 632–637.
- (28) Wu, H.-F.; Brodbelt, J. S. *Inorg. Chem.* **1995**, *34*, 615–621.
- (29) Liou, C.-C.; Isbell, J.; Wu, H.-F.; Brodbelt, J. S.; Bartsch, R. A.; Lee, J. C.; Hallman, J. L. *J. Mass Spectrom.* **1995**, *30*, 572–580.
- (30) Alvarez, E. J.; Wu, H.-F.; Liou, C.-C.; Brodbelt, J. *J. Am. Chem. Soc.* **1996**, *118*, 9131–9138.
- (31) Glendening, E. D.; Feller, D.; Thompson, M. A. *J. Am. Chem. Soc.* **1994**, *116*, 10657–10669.
- (32) More, M. B.; Glendening, E. D.; Ray, D.; Feller, D.; Armentrout, P. B. *J. Phys. Chem.* **1996**, *100*, 1605–1614.
- (33) Ray, D.; Feller, D.; More, M. B.; Glendening, E. D.; Armentrout, P. B. *J. Phys. Chem.* **1996**, *100*, 16116–16125.
- (34) Hill, S. E.; Glendening, E. D.; Feller, D. *J. Phys. Chem. A* **1997**, *101*, 6125.
- (35) More, M. B.; Ray, D.; Armentrout, P. B. *J. Phys. Chem. A* **1997**, *101*, 831–839.
- (36) More, M. B.; Ray, D.; Armentrout, P. B. *J. Phys. Chem.*, in press.
- (37) More, M. B.; Ray, D.; Armentrout, P. B. *J. Phys. Chem. A* **1997**, *101*, 7007–7017.
- (38) Glendening, E. D.; Feller, D. *J. Am. Chem. Soc.* **1996**, *118*, 6052–6059.
- (39) Hehre, W. J.; Ditchfield, R.; Pople, J. A. *J. Chem. Phys.* **1972**, *56*, 2257–2261.
- (40) Hariharan, P. C.; Pople, J. A. *Theor. Chem. Acta* **1973**, *28*, 213.
- (41) Clark, T.; Chandrasekhar, J.; Spitznagel, G. W.; Schleyer, P. v. R. *J. Comput. Chem.* **1983**, *4*, 294.
- (42) Hay, P. J.; Wadt, W. R. *J. Chem. Phys.* **1985**, *82*, 299–310.
- (43) Del Bene, J. E.; Mettee, H. D.; Frisch, M. J.; Luke, B. T.; Pople, J. A. *J. Phys. Chem.* **1983**, *87*, 3279–3282.
- (44) Frisch, M. J.; Trucks, G. W.; Head-Gordon, M.; Gill, P. M. W.; Wong, M. W.; Foresman, J. B.; Johnson, B. G.; Schlegel, H. B.; Robb, M. A.; Replogle, E. S.; Gomperts, R.; Andres, J. L.; Raghavachari, K.; Binkley, J. S.; Gonzalez, C.; Martin, R. L.; Fox, D. J.; Defrees, D. J.; Baker, J.; Stewart, J. J. P.; Pople, J. A. *Gaussian 92*, Revision C.; Gaussian, Inc.: Pittsburgh, PA, 1992.
- (45) Frisch, M. J.; Trucks, G. W.; Schlegel, H. B.; Gill, P. M. W.; Johnson, B. G.; Robb, M. A.; Cheeseman, J. R.; Keith, T.; Petersson, G. A.; Montgomery, J. A.; Raghavachari, K.; Al-Laham, M. A.; Zakrzewski, V. G.; Ortiz, J. V.; Foresman, J. B.; Cioslowski, J.; Stefanov, B. B.; Nanayakkara, A.; Challacombe, M.; Peng, C. Y.; Ayala, P. Y.; Chen, W.; Wong, M. W.; Andres, J. L.; Replogle, E. S.; Gomperts, R.; Martin, R. L.; Fox, D. J.; Binkley, J. S.; Defrees, D. J.; Baker, J.; Stewart, J. P.; Head-Gordon, M.; Gonzalez, C.; Pople, J. A. *Gaussian 94*, Revision D.1; Gaussian, Inc.: Pittsburgh, PA, 1995.
- (46) Boys, S. F.; Bernardi, F. *Mol. Phys.* **1970**, *19*, 553.
- (47) Glendening, E. D.; Feller, D. *J. Phys. Chem.* **1995**, *99*, 3060–3067.
- (48) Glendening, E. D.; Feller, D. *J. Phys. Chem.* **1996**, *100*, 4790–4797.
- (49) Feller, D.; Aprà, E.; Nichols, J. A.; Bernholdt, D. E. *J. Chem. Phys.* **1996**, *105*, 1940–1950.
- (50) Dunning, T. H., Jr. *J. Chem. Phys.* **1989**, *90*, 1007–1023.
- (51) Kendall, R. A.; Dunning, T. H., Jr.; Harrison, R. J. *J. Chem. Phys.* **1992**, *96*, 6796–6806.
- (52) Feller, D.; Glendening, E. D.; Woon, D. E.; Feyereisen, M. W. *J. Chem. Phys.* **1995**, *103*, 3526–3542.
- (53) Glendening, E. D.; Streitwieser, A. *J. Chem. Phys.* **1994**, *100*, 2900–2909.
- (54) Hay, B. P.; Rustad, J. R.; Zipperer, J. P.; Wester, D. W. *J. Mol. Struct.: THEOCHEM* **1995**, *337*, 39–47.